

## Effect of Cinnamate Comonomers on the Dental Formulation Properties

Emil C. Buruiana, Florentina Jitaru, Violeta Melinte, Tinca Buruiana

Photochemistry and Polyaddition Department, Petru Poni Institute of Macromolecular Chemistry, Romanian Academy, Iasi 700487, Romania

Correspondence to: E. C. Buruiana (E-mail: emilbur@icmpp.ro)

**ABSTRACT:** This study reports the synthesis and characterization of two urethane dimethacrylates containing poly(ethylene oxide) or poly(propylene oxide) segment and cinnamate pendant moieties to be formulated in dental resin composites.  $^1\text{H}$  NMR,  $^{13}\text{C}$  NMR, and Fourier transform infrared spectroscopies, gel permeation chromatography, electrospray ionization-mass spectroscopy, and thermogravimetric measurements confirmed their structure, whereas the photopolymerization evolution of oligodimethacrylates relating to a low-molecular-weight dicinnamate methacrylate under ultraviolet irradiation was investigated by photo-differential scanning calorimeter, monitoring the degree of conversion (DC) and polymerization rate. The photopolymerization results reveal that the investigated derivatives display a good photoreactivity (DC:  $\sim 70\%$ ) during the formation of crosslinked polymers, the DC depending especially on the sample viscosity. The polymerization shrinkage for several mixtures including the urethane oligocinnamates (20 wt %) and diglycidyl methacrylate of bisphenol A/triethyleneglycol dimethacrylate system in the absence of filler was determined, the obtained values being in the range of 6.1–8.2 vol %. For few cured specimens incorporating quartz filler (75 wt %), water sorption/solubility, contact angle, and mechanical parameters were measured to establish if such monomers could be of interest in dentistry. © 2012 Wiley Periodicals, Inc. *J. Appl. Polym. Sci.* 000: 000–000, 2012

**KEYWORDS:** cinnamate oligomers; photopolymerization; dental polymers; composites

Received 9 January 2012; accepted 22 April 2012; published online

DOI: 10.1002/app.37942

### INTRODUCTION

Most composite materials frequently encountered in conservative dentistry continue to use the diglycidyl methacrylate of bisphenol A (Bis-GMA), as the main component of the photopolymerizable organic phase.<sup>1–3</sup> Owing to its high viscosity (540–1200 Pa s),<sup>4</sup> this dimethacrylate needs dilution with large proportions of low-viscosity monomers such as triethyleneglycol dimethacrylate (TEGDMA) or ethyleneglycol dimethacrylate to achieve a higher filler loading (up to 80 wt %) for a successful dental composite. Previous studies have been shown that the composite properties can be tailored according to the wanted application through an appropriate choice of the monomers implied in the formation of interpenetrating polymer network as well as by varying the inorganic filler (nature, size, loading, shape, distribution, adhesion, etc.), the latter strategy revolutionizing practically the dental materials arena in the last decade.<sup>5–7</sup> In spite of numerous advantages reported in the literature, the major deficiencies of such composites are still related to the high-polymerization shrinkage (PS)<sup>7,8</sup> and incomplete polymerization of the monomers that cause, with time, a deterioration of the physical/mechanical properties in the final

materials.<sup>9,10</sup> Further efforts were made to diminish the aforementioned drawbacks through the development of novel monomeric systems such as modified Bis-GMA,<sup>3</sup> liquid crystalline (LC) monomers,<sup>11–13</sup> dendritic methacrylates,<sup>14</sup> bis-acrylamides,<sup>15</sup> ormocers,<sup>16</sup> or more recently, siloranes,<sup>17,18</sup> together with strongly acidic methacrylates that adhere on enamel and dentin.<sup>19</sup> Other studies have been evaluated the family of urethane dimethacrylates (UDMAs) for their capability to improve the properties of dental restorative materials,<sup>20,21</sup> owing to the relatively high molecular weight, crosslinking density, and cohesive energy density generated by the urethane structure.<sup>22</sup> Distinctively, the last novel product (Kalore/Venus Diamond) that bears urethane groups is characterized by a very small volumetric shrinkage.<sup>23</sup>

Within this context, several urethane (di)methacrylates have been developed in our group including the reactive acid-functionalized oligomers<sup>24,25</sup> and nonacid ones,<sup>26</sup> LC monomers,<sup>13</sup> and Bis-GMA analogous,<sup>13,27</sup> as well as photopolymerizable polyalkenoates,<sup>28</sup> to investigate the influence of chemical structure and composition on the photopolymerization process in some dental formulations. Additionally, the study of the

© 2012 Wiley Periodicals, Inc.

properties of photo-cured networks resulted from the above monomers was essential to understand their behavior in such resin composites. On this line, there are few reports devoted to physical studies of the effect of spacer length between the methacrylate groups on the final properties of dental materials.<sup>29</sup> As has been pointed out, the reactivity of monomers increases with increasing the length and the flexibility of the spacer.<sup>30,31</sup> In fact, the incorporation of the flexible spacer in urethane dimethacrylates was inspired of the qualities of poly(ethylene glycol) (PEG) derivatives considered as viable alternative to 2-hydroxyethyl methacrylate (HEMA) in dental composites,<sup>32</sup> as well as those of the poly(propylene glycol) (PPG) chain which is a component of the Fotofil® product in dental practice.<sup>33</sup>

In this contribution, we focused our attention on synthesizing oligodimethacrylates with photosensitive cinnamate groups, which were further reacted with conventional dental monomers (Bis-GMA and TEGDMA) to create polymeric networks intended for dental composites, whose properties were also examined. It should be emphasized that the cinnamate groups from polymers may undergo photoisomerization/photodimerization reactions under ultraviolet (UV) irradiation.<sup>34,35</sup> On the other hand, the choice of cinnamate derivatives for testing in dental resin composites is motivated by the fact that such structures are nontoxic and can present antiseptic, antitumoral, or anaesthetic activity,<sup>36,37</sup> and are, therefore, suitable for the preparation of functional biomaterials.

## EXPERIMENTAL

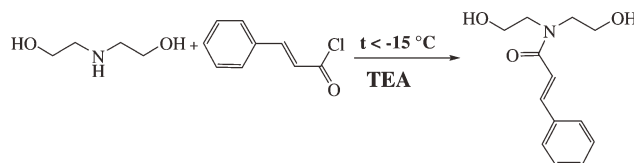
### Materials

Diethanolamine, cinnamoyl chloride, triethyl amine, PEG ( $M_{\text{PEG}} = 400$  g/mol), PPG ( $M_{\text{PPG}} = 425$  g/mol), poly(tetramethylene oxide) (PTHF,  $M_{\text{PTHF}} = 1000$  g/mol), isophorone diisocyanate (IPDI), HEMA, Bis-GMA, TEGDMA, and dibutyltin dilaurate were purchased from Sigma-Aldrich Chemical (Taufkirchen, Germany) and used without further purification. The initiators used were Darocur TPO and Irgacure 651 from Ciba (Basel, Switzerland), camphorquinone (CQ) and 4-(dimethylamino)-phenylacetic acid (DMPheAA) from Sigma-Aldrich Chemical, whereas the filler used was quartz (silicon dioxide nanopowder, granulation 10–20 nm from TEM) from Sigma-Aldrich Chemical.

### Synthesis

For the preparation of cinnamate difunctional oligomers, first, the synthesis of *N,N*-bis(2-hydroxyethyl) cinnamamide (C-DOH) as intermediate was performed (Scheme 1). Thus, a solution of 3.15 g (0.03 mol) diethanolamine in anhydrous tetrahydrofuran (THF) (10 mL) was cooled to  $-20^{\circ}\text{C}$  and then, 5 g (0.03 mmol) cinnamoyl chloride in 10 mL THF was dropwise added in the presence of 4.33 mL (0.03 mol) triethyl amine, at such a rate that the reaction temperature was maintained at  $-20^{\circ}\text{C}$ . After finishing the drip, the temperature of the mixture was arisen at room temperature and kept under stirring for 48 h. Finally, the solution was filtrated, and the solvent was evaporated under reduced pressure.

$^1\text{H}$  NMR (400 MHz,  $\text{CDCl}_3$ ,  $\delta$  ppm): 7.7–7.5 (d, 1H,  $-\text{CH}=\text{CH}-\text{Ar}$ ); 7.5–7.2 (m, 5H, Ar H); 6.45 (d, 1H,



**Scheme 1.** Synthesis of the reaction intermediate C-DOH.

$-\text{CO}-\text{CH}=\text{CH}-\text{Ar}$ ); 5.12 (s, 2H, OH); 3.8 (t, 4H,  $\text{HO}-\text{CH}_2-\text{CH}_2-\text{N}$ ); 3.6 (t, 4H,  $\text{HO}-\text{CH}_2-\text{CH}_2-\text{N}$ ).

For the synthesis of cinnamate dimethacrylate oligomers ( $\text{O}_1\text{-DMA}$ ,  $\text{O}_2\text{-DMA}$ ), PEG or PPG macrodiols were used, together with IPDI, C-DOH, and HEMA, employing the following molar ratio: PEG(PPG): IPDI: C-DOH: HEMA = 0.5 : 2 : 0.5 : 2. Considering the similar synthetic pathway, here we describe only the preparative steps involved in the obtaining of  $\text{O}_1\text{-DMA}$ . Hereby, 1 g PEG (2.5 mmol) was degassed in vacuum for 2 h ( $100^{\circ}\text{C}$ ). Then, the system temperature was reduced to  $50^{\circ}\text{C}$  and 2.16 mL (10 mmol) IPDI was added, the mixture being stirred at  $60^{\circ}\text{C}$  for 4 h in the presence of catalytic amount of dibutyltin dilaurate. After that, the temperature was reduced to  $40^{\circ}\text{C}$  and 0.59 g (2.5 mmol) C-DOH dissolved in anhydrous THF was added, the reaction being continued for 2 h. At the same temperature ( $40^{\circ}\text{C}$ ), 1.4 mL (10 mmol) of HEMA was added and the mixture was stirred for 10 h. The course of the reaction was pursued through the infrared absorption of the isocyanate stretching band at  $2260\text{ cm}^{-1}$ , the reaction being considered complete after the disappearance of this band from the FTIR spectrum. For removing the catalyst, the cinnamate dimethacrylate oligomers were dissolved in methylene chloride and the solution was stirred with 2% HCl solution (4 : 1 v/v) at room temperature. After the separation of the organic phase and the evaporation of solvent, the oligomers were collected as pale yellow viscous liquids.

**$\text{O}_1\text{-DMA}$ :**  $\eta = 48.2$  Pa s.  **$\text{O}_2\text{-DMA}$ :**  $^1\text{H}$  NMR (400 MHz,  $\text{CDCl}_3$ ,  $\delta$  ppm): 7.7 (d, 1H,  $-\text{CH}=\text{CH}-\text{Ar}$ ); 7.45–7.2 (m, 5H, Ar H); 6.7 (d, 1H,  $-\text{CO}-\text{CH}=\text{CH}-\text{Ar}$ ); 6.14 (d, 4H,  $\text{CH}_2=\text{C}$  in *trans*-position relative to  $\text{CH}_3$  unit from HEMA); 5.56 (s, 4H,  $\text{CH}_2-\text{C}$  in *cis*-position relative to  $\text{CH}_3$  unit from HEMA); 4.4–4.2 (m, 20H,  $\text{COO}-\text{CH}_2$  and  $\text{NH}-\text{COO}-\text{CH}_2-\text{CH}_2$ ); 3.7 (m, 6H,  $\text{CH}_2-\text{CH}(\text{CH}_3)-\text{O}$ ); 3.6 (m, 12H,  $\text{CH}_2-\text{CH}(\text{CH}_3)-\text{O}$ ); 3.4–3.2 (m, 8H,  $\text{CH}_2-\text{NH}-\text{COO}$ ); 1.95 (s, 12 H,  $\text{CH}_3$  from HEMA); 1.71–0.7 (m, 81 H, protons from isophorone unit and  $\text{CH}_2-\text{CH}(\text{CH}_3)-\text{O}$ ).

$^{13}\text{C}$  NMR (400 MHz,  $\text{CDCl}_3$ ,  $\delta$  ppm):  $\text{C}_1$ , 47.11;  $\text{C}_2$ , 46.4;  $\text{C}_3$ , 31.87;  $\text{C}_4$ , 46.40;  $\text{C}_5$ , 36.49;  $\text{C}_6$ , 41.89;  $\text{C}_7$ , 35.16;  $\text{C}_8$ , 27.71;  $\text{C}_9$ , 23.32;  $\text{C}_{10}$ , 55.03;  $\text{C}_{\text{h,p}}$ , 156.74;  $\text{C}_{\text{g,o}}$ , 155.54 ppm (from isophorone diurethane);  $\text{C}_a$ , 126.14;  $\text{C}_b$ , 136.19;  $\text{C}_c$ , 17.18;  $\text{C}_d$ , 167.75 ppm (methacrylate);  $\text{C}_e$ , 70.01;  $\text{C}_{\text{f,q}}$ , 62.68 ppm (ester); 72.0–76.2 ppm ( $\text{C}_{\text{i,k}}$ ) and 18.42 ( $\text{C}_m$ ) from PPG; 167.27 ppm ( $\text{C}_s$ , from cinnamide); 143.2 and 116.11 ( $\text{C}_v$ ,  $\text{C}_u$ ); 126.00 ppm (aromatic C).  $\eta = 55.7$  Pa s.

The methacrylate monomer with cinnamate groups *N,N*-bis( $\beta$ -cinnamoyloxyethyl)-*N'*-methacryloyloxyethyl urea (DC-MA) was prepared according to the previously reported method.<sup>38</sup>  $^1\text{H}$  NMR ( $\text{CDCl}_3$ ,  $\delta$  ppm): 7.7 (d, 2H,  $-\text{CH}=\text{CH}-\text{Ar}$ ); 7.6–7.3

(m, 10H, Ar H); 6.45 (d, 2H,  $-\text{CO}-\text{CH}=\text{CH}-\text{Ar}$ ); 6.15 (d, 1H,  $\text{CH}_2=\text{C}$  in *trans*-position relative to  $\overline{\text{C}}\text{H}_3$  unit); 5.55 (s, 1H,  $\text{CH}_2=\text{C}$  in *cis*-position relative to  $\overline{\text{C}}\text{H}_3$  unit); 4.5–4.3 (m, 6H,  $\text{CH}_2-\text{OCO}$ ), 3.9–3.4 (m, 6H,  $\text{CH}_2-\text{NH}-\text{CO}$  and  $\text{N}-\text{CH}_2-\text{CH}_2$ ), 1.95 (s, 3H,  $\text{CH}_3$ ).  $\eta = 19.3 \text{ Pa s}$ .

### Characterization

The oligodimethacrylates structures were verified by  $^1\text{H}$  NMR and FTIR spectroscopy using a Bruker Avance DRX 400 spectrometer and a Bruker Vertex 70 FTIR spectrophotometer, respectively. Viscosity measurements of the urethane dimethacrylates were determined with a Brookfield cone and plate viscometer at room temperature. The test was run at spindle speeds of 6 and 12 rpm and the viscosity readings obtained were recorded and expressed as Pascal second (Pa s). Differential scanning photocalorimetry studies were performed on a DuPont 930 apparatus with a double heat differential calorimeter 912, calibrated with indium metal standard according to the literature.<sup>39</sup>

The average molecular weight was determined in chloroform by gel permeation chromatography (GPC) analysis on a PLEMD 950 apparatus equipped with two PL gel-mixed columns using polystyrene standards. Mass spectrometry (MS) results were obtained using an Agilent 6520 Series Accurate-Mass Quadrupole Time-of-Flight LC/MS. The solutions were introduced into the electrospray ionization (ESI) source via a syringe pump at a flow rate of 0.2 mL/min. After optimization of the Q/TOFMS parameters, they were set as follows: ESI (positive ion mode), drying gas ( $\text{N}_2$ ) flow rate, 7.0 L/min; drying gas temperature, 325°C; nebulizer pressure, 35 psig; capillary voltage, 4000 V; fragmentation voltage, 200 V, and the full-scan mass spectra of the investigated compounds being acquired in the  $m/z$  range of 100–3000. The mass scale was calibrated using the standard calibration procedure and compounds were provided by the manufacturer. Data were collected and processed using Mass Hunter Workstation software.

Thermal degradation of the polymers was performed using a Jupiter STA 449F1 thermogravimetric balance (Netzsch, Germany). Samples (mass ranging from 7 to 10 mg) were heated from 30 to 600°C, at rates of 10°C/min. Nitrogen (purity, 99.99%) was used as a carrier (flow rate, 50 mL/min) and protective purge for the thermobalance (flow rate, 20 mL/min). The samples were heated in an open  $\text{Al}_2\text{O}_3$  crucible using  $\text{Al}_2\text{O}_3$  as reference material. Data were processed with Proteus® software.

A standard high-pressure mercury lamp with 4.5 mW/cm<sup>2</sup> light intensity was used for UV irradiating the sample ( $1.5 \pm 0.5$  mg) in the presence of Darocur TPO, Irgacure 651, or CQ/DMPheAA as the initiator system, using differential scanning calorimeter (DSC) DuPont standard pans. A polyethyleneterephthalate (Mylar® film) was used to cover the composition in the photo-DSC pan, so as to prevent the diffusion of atmospheric oxygen into the sample. The measurements were performed in an isothermal mode and irradiation started after 1 min of equilibration. The heat flux as a function of reaction time was monitored using photo-DSC under isothermal conditions, both the rate of polymerization and the conversion being calculated as a

function of time.<sup>40</sup> The PS of cured and uncured specimens tested in the present study was determined by the density bottle method at room temperature.<sup>41</sup> Photocurable pastes for volumetric shrinkage measurement were formulated using a weight ratio of cinnamate oligomer : Bis-GMA : TEGDMA : CQ : DMPheAA of 20 : 48.5 : 30 : 0.5 : 1. The specimens in the form of small cylinders (approximately, 0.2 g in weight) obtained after photopolymerization under visible-light irradiation (450–470 nm) using LED curing light (DEMETRON A2; 800 mW/cm<sup>2</sup>) for 30 s on each side were placed in a density bottle of 20 cm<sup>3</sup> volume containing distilled water ( $q_{\text{H}_2\text{O}}$  at 25°C = 0.99707 g/cm<sup>3</sup>). A Partner balance (accuracy =  $\pm 0.000001$  g) was used. Three successive measurements for all tested composites were performed. The PS was determined separately for each specimen using the eq. (1):

$$\text{Polymerization shrinkage} = \frac{d_{\text{cured}} - d_{\text{uncured}}}{d_{\text{cured}}} \times 100 \quad (1)$$

where  $d$  is the density of the formulation.

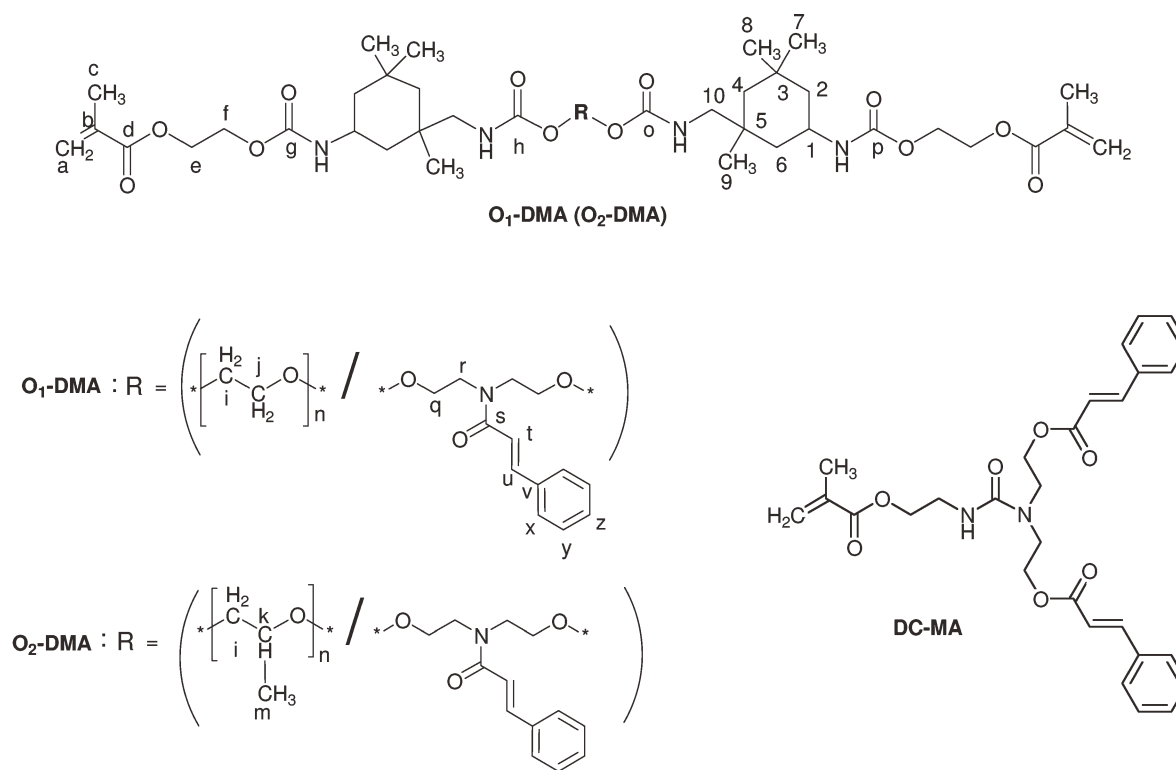
The filled resin composites for contact angle, water sorption, and water solubility determinations were prepared by using 25 wt % organic matrix and 75 wt % inorganic filler (quartz). The organic resin matrix consisted of cinnamate oligomer : Bis-GMA : TEGDMA mixture (20 : 48.5 : 30 wt/wt) and CQ/DMPheAA as the initiator system. The static water contact angle measurements were made on disk-shaped specimens ( $15 \pm 0.1$  mm diameter,  $1 \pm 0.1$  mm thickness) using goniometer KSV Cam 200. Two microliter droplets of double-distilled water was placed on the disk specimen surface, the average contact angle being calculated starting from at least 10 separate measurements. The water sorption and water solubility were determined<sup>42</sup> by preparing four disk specimens of reduced dimensions ( $15 \pm 0.1$  mm diameter,  $1 \pm 0.1$  mm thickness) for each group of mixtures, using a Teflon split ring mold between two glass plates covered with polyethylene film. The composites were preconditioned over a desiccant containing calcium sulfate at 37°C until their weight remains constant (initial weight  $m_1$ ). Further, specimens were placed in distilled water at 37°C for different time intervals and then removed from the water, lightly blotted with a paper to eliminate the surface-adherent water, and weighed. After 3 weeks ( $m_2$ ), specimens were placed into a desiccator with calcium sulfate and dried at 37°C until their weight was constant again ( $m_3$ ). The water solubility for each sample was determined using eq. (2):

$$\text{Water solubility (wt\%)} = \frac{m_1 - m_3}{m_1} \times 100 \quad (2)$$

whereas the water sorption was calculated employing eq. (3):

$$\text{Water sorption (wt\%)} = \frac{m_2 - m_3}{m_1} \times 100 \quad (3)$$

Compressive strength (CS) and diametral tensile strengths (DTS) were measured using a Shimadzu AGS-J testing machine, with a 5 kN load cell. Specimens for the CS and DTS tests were prepared by mixing the components using a metal spatula and



**Scheme 2.** Structure of oligodimethacrylates (O<sub>1</sub>-DMA and O<sub>2</sub>-DMA) and DC-MA with cinnamate groups.

filling five metal cylinder molds, all of 8 mm in height and 4 mm in diameter, which were prewaxed to prevent material adhesion. A crosshead speed of 1 mm/min was applied in these tests. The CS was calculated from the equation  $CS = P/\pi r^2$ , where  $P$  is the load at fracture and  $r$  the radius of the sample cylinder. DTS was calculated from the relationship  $DTS = 2P/\pi dt$ , where  $d$  is the diameter and  $t$  the thickness, respectively, of the cylinder.

## RESULTS AND DISCUSSION

### Synthesis and Spectral Characterization of Cinnamate Dimethacrylate Oligomers

The structures of the cinnamate monomers synthesized in this study are shown in Scheme 2. The first urethane dimethacrylates of oligomeric type (O<sub>1</sub>-DMA and O<sub>2</sub>-DMA) were prepared by a classical addition reaction between PEG ( $M_{\text{PEG}} = 400$  g/mol) or PPG ( $M_{\text{PPG}} = 425$  g/mol), IPDI, and C-DOH (Scheme 1), subsequently reacted with HEMA, taken into a molar ratio of 0.5 : 2 : 0.5 : 2. Although the reaction of isocyanate with hydroxyl groups from monomers is performed by minimizing the occurrence of side reactions, it does not provide strict control over the composition of the resulting product, but the simplicity of the procedure, widely exploited to prepare polyurethanes,<sup>43</sup> may be advantageous in applications where a narrow polydispersity is optional. The reason for the validity of the oligomeric structures represented in an idealized form (HEMA-IPDI-[PEG/C-DOH]-IPDI-HEMA) will be discussed later. For comparison, a low-molecular-weight methacrylate, namely DC-MA, was also prepared from 2-isocyanatoethyl methacrylate and diethanolamine to afford *N,N*-bis( $\beta$ -hydroxyethyl)-*N'*-methacry-

loyloxyethyl urea, which was then converted to DC-MA by reacting with cinnamoyl chloride according to the previous data.<sup>38</sup> The chemical structure of the cinnamate dimethacrylates was confirmed by <sup>1</sup>H NMR and FTIR spectroscopies. Thus, the <sup>1</sup>H NMR study on O<sub>1</sub>-DMA [Figure 1(a)] indicates the presence of peaks at 7.5–7.3 ppm attributed to the aromatic protons, whereas the unsaturated protons from cinnamate can be identified at 7.69 and 6.8 ppm. Other signals belong to the unsaturated protons from methacrylate (6.14 and 5.6 ppm), methylene protons from the ester-urethane groups and the ester unit of HEMA (4.4–4.2 ppm), methyne protons close to the urethane groups (3.79 ppm), methylene protons from PEG (3.67 ppm), the methylene protons neighboring the urethane groups (2.9 ppm), methyl protons from HEMA (1.95 ppm), and protons on the isophorone cycle (1.7–0.7 ppm). Similar profile was observed for O<sub>2</sub>-DMA, excepting the methyne protons (3.8 ppm) and methyl protons from PPG which are overlapped with protons from isophorone. Investigation of the above structures by <sup>13</sup>C NMR gave significant information. Figure 1(b) shows the <sup>13</sup>C NMR spectrum for O<sub>1</sub>-DMA (Scheme 2), which exhibits characteristic signals for carbon atoms from isophorone diurethane (C<sub>1</sub>, 47.57; C<sub>2</sub>, 46.95; C<sub>3</sub>, 31.78; C<sub>4</sub>, 46.95; C<sub>5</sub>, 36.33; C<sub>6</sub>, 44.57; C<sub>7</sub>, 35.00; C<sub>8</sub>, 27.75; C<sub>9</sub>, 23.16; C<sub>10</sub>, 54.86; C<sub>h,p</sub>, 155.63; C<sub>g,o</sub>, 155.54 ppm), methacrylate (C<sub>a</sub>, 127.92; C<sub>b</sub>, 136.03; C<sub>c</sub>, 18.26; C<sub>d</sub>, 167.65 ppm), and ester functions (C<sub>e</sub>, 69.57; C<sub>f</sub>, 62.91 ppm). PEG gives signals at 70.50 ppm (C<sub>i,j</sub>), whereas the carbon atoms from cinnamide appear at 167.15 ppm (C<sub>s</sub>). Other three signals owing to C<sub>t</sub>, C<sub>u</sub>, and aromatic carbons can be observed at 143.2, 116, and 126.00 ppm, respectively.



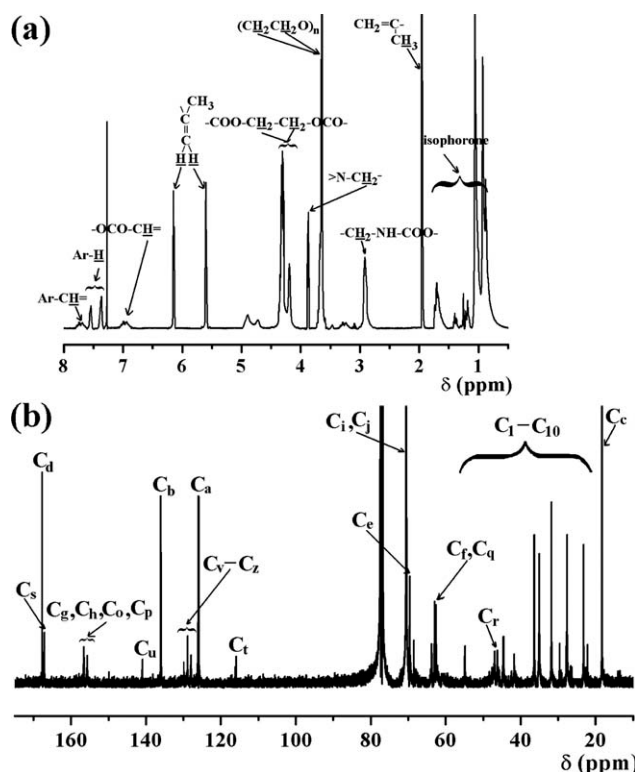


**Figure 1.**  $^1\text{H}$  NMR (a) and  $^{13}\text{C}$  NMR (b) spectrum of poly(ethylene oxide) urethane dimethacrylate with cinnamate groups ( $\text{O}_1$ -DMA) in  $\text{CDCl}_3$ .

In connection, the FTIR spectra shown in Figure 2 sustain the structure of the synthesized dimethacrylates. The characteristic absorption bands of the urethane NH, C—H, and carbonyl groups appeared at 3334, 2954, and  $1718\text{ cm}^{-1}$ , respectively, whereas the band of C=C double bond from methacrylate and cinnamate units can be viewed at  $1640$  and  $816\text{ cm}^{-1}$ . UV spectroscopy has also revealed a strong absorption band with maximum at about 278 nm, attributed to the  $\pi$ - $\pi^*$  transition from the cinnamate moiety.

To further confirm the oligomeric character and chemical structure of the urethane dimethacrylates, electrospray ionization tandem mass spectroscopy (ESI-MS) and GPC analysis were carried out on our samples and the commercial PEG (PPG) was selected for the synthesis. In the ESI-MS spectra of PEG, PPG,  $\text{O}_1$ -DMA, and  $\text{O}_2$ -DMA in THF, the appearance of characteristic mass signals can be detected. Thus, in the case of PEG [Figure 3(a)], two Gaussian distributions for cationized species ( $\text{K}^+$  PEG and  $\text{Na}^+$  PEG) were observed, whereas PPG (Figure 4(a)) gave rise to a single Gaussian distribution ( $\text{Na}^+$  PPG). On the first curves, there are seven signals separated by 44 Da that correspond to a number of ethylene oxide units varying between 6 and 12. The most abundant signal ( $453.22$ ;  $437.2$ ) suggests the existence of nine units of PEG (molecular weight, 414) assigned to the  $\text{K}^+$  and  $\text{Na}^+$  PEG adduct, respectively. Then, by analyzing the recorded PPG Gaussian curve, we observed approximately six signals, all separated by 58 Da that correspond to 5–10 propylene oxide units. The abundant signal ( $447.31$ ) corresponding

to seven units of propylene oxide (molecular weight, 424) belongs to  $\text{Na}^+$  PPG adduct.

In the light of these results, ESI-MS spectra of  $\text{O}_1$ -DMA [Figure 3(b)] and  $\text{O}_2$ -DMA [Figure 4(b)] sustain the presence of cationized species ( $\text{Na}^+$  PEG or  $\text{K}^+$  PPG) characterized by the molecular weights of 1157.71 and 1167.77, corresponding to seven monomeric units of PEG and five units of PPG, respectively. Therefore, both dimethacrylates contain either PEG or PPG chain, as illustrated by the most probable chemical structure shown in Scheme 2. These results seem to be in a good agreement with the molar ratio used in the synthesis of urethane oligodimethacrylates.

Complementary, a comparison between GPC curves of  $\text{O}_1$ -DMA,  $\text{O}_2$ -DMA, and precursor oligoether diols is shown in Figures 3(a) and 4(a) (inset). In the PEG (PPG) chain extension experiment with IPDI, C-DOH, and HEMA, the molecular weight ( $M_{n,\text{GPC}}$ ) of the  $\text{O}_1$ -DMA sample increased from 400 to 1043, whereas for  $\text{O}_2$ -DMA this increased from 425 to 1052. Therefore, in both cases, complete consumption of the initial partners was demonstrated through a clear shift to a higher molecular weight as observed from the GPC traces. Thus, we conclude that the presence of a unimodal distribution pattern in the GPC analysis is an indicator for the lack of other molecular species.

Additionally, evaluation of the thermal stability of monomers by thermogravimetric analysis proved that the cinnamate dimethacrylates are stable up to  $180$ – $200^\circ\text{C}$  in an atmosphere of nitrogen (Figure 5). Besides their above-discussed characteristics, our monomers have good solubility in conventional dimethacrylates (Bis-GMA, UDMA, and TEGDMA) and in organic solvents as chloroform, THF, and methylene chloride. Although viscosity of the cinnamate monomers ( $19$ – $55\text{ Pa s}$ ) is lower than that of Bis-GMA, in our experiments this parameter was reduced by adding TEGDMA as reactive diluent.

### Photopolymerization Study

In a first assessment of these new monomers, the photopolymerization kinetics has been analyzed by photo-DSC to establish if the chemical structure is the determining factor for the

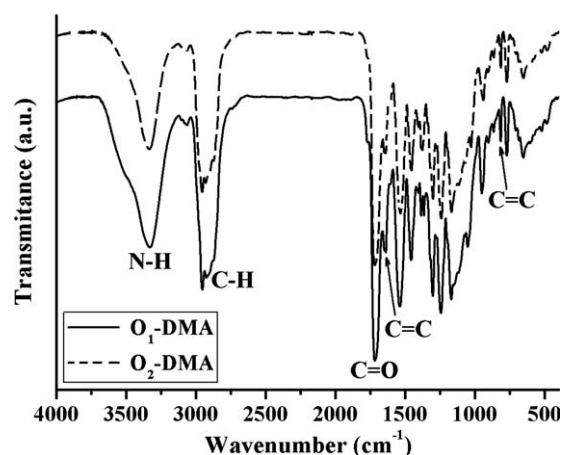


**Figure 2.** FTIR spectra of oligodimethacrylates with cinnamate groups.

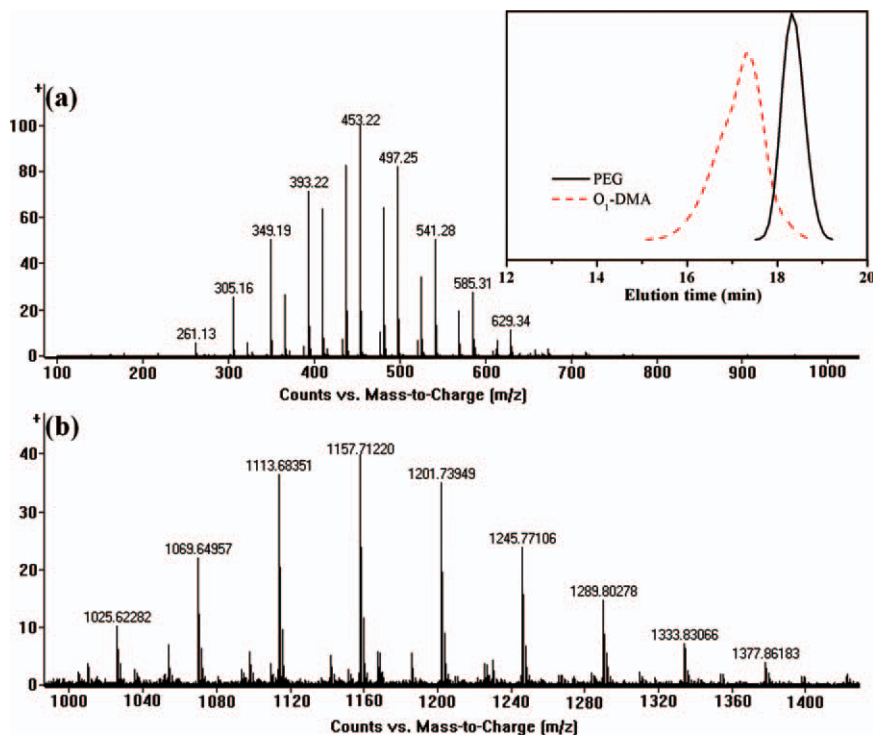


**Figure 3.** ESI-MS for PEG (a) and  $O_1$ -DMA (b) and their GPC curves (inset). [Color figure can be viewed in the online issue, which is available at [wileyonlinelibrary.com](http://wileyonlinelibrary.com).]

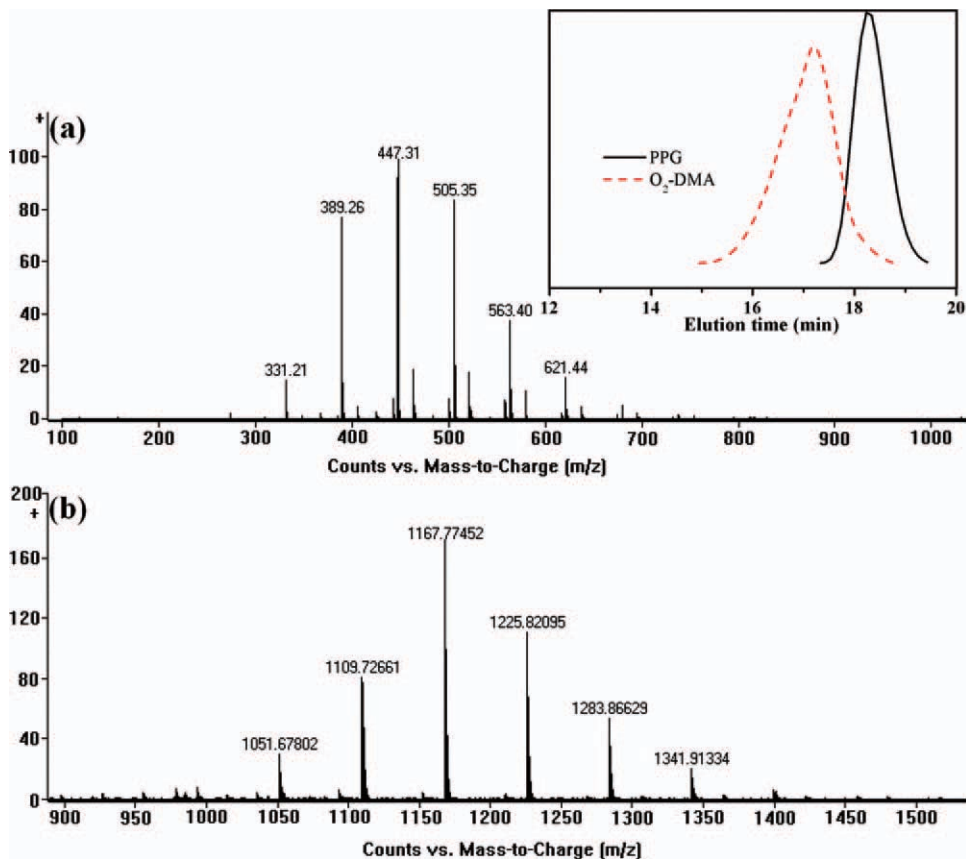


**Figure 4.** ESI-MS for PPG (a) and  $O_2$ -DMA (b) and their GPC curves (inset). [Color figure can be viewed in the online issue, which is available at [wileyonlinelibrary.com](http://wileyonlinelibrary.com).]

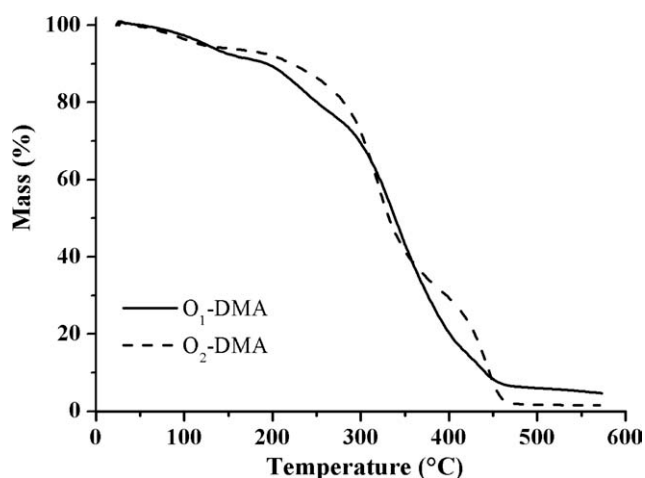


Figure 5. TG curves of the O<sub>1</sub>-DMA and O<sub>2</sub>-DMA dimethacrylates.

polymerization photoreactivity. For this purpose, the time to attain the maximum polymerization heat ( $t_{\max}$ ), the double-bond conversion to single bonds after polymerization and the polymerization rate ( $R_p$ ) were determined at room temperature. Under given conditions of photopolymerization (exposure to UV light in the presence of 1 wt % Darocour TPO as photoinitiator), each monomer was polymerized up to the formation of a hard polymer matrix. As shown in Figure 6(a), the degree of conversion (DC) of the methacrylate C=C bond attained after 5 min of irradiation significantly increased from urethane oligocinnamates (DC = 70%) to the low-molecular-weight methacrylate DC-MA (DC, 94%) as photopolymerization occurred (Table I). Moreover, the quantification of the photoreactivity, reflected by the maximum polymerization rate ( $R_{\max}^p$ ) [Figure 6(b)] evidenced that the highest polymerization rate value was obtained in the case of O<sub>1</sub>-DMA for which the rate at the peak maximum was found to be  $R_{\max}^p = 0.101 \text{ s}^{-1}$ . For O<sub>2</sub>-DMA, the value of the maximum polymerization rate slightly decreased to  $R_{\max}^p = 0.093 \text{ s}^{-1}$ . This modest variation in the sample photoreactivity may be ascribed to the viscosity effect of the photopolymerizable derivatives that influence the macromolecular chain mobility.<sup>44</sup> A contradictory situation is, however, noticed in case of the monomethacrylate with two cinnamate groups (DC-MA), which although has a lower viscosity than that measured for the oligocinnamates, presented a lower maximum polymerization rate ( $R_{\max}^p = 0.052 \text{ s}^{-1}$ ). Such finding may be related to the fact that sometimes, a decrease in viscosity generates low-polymerization rates compensated by higher final conversions (e.g., the case observed at the free radical homopolymerization of Bis-GMA, UDMA, or TEGDMA, when UDMA showed the highest polymerization rate, and TEGDMA had the highest final conversion<sup>45</sup>).

A modification of the photopolymerizable composition through the addition of another oligodimethacrylate (O<sub>3</sub>-DMA based on PTHF of 1000 average molecular weight, Scheme 3)<sup>46</sup> as comonomer in the combination O<sub>1</sub>-DMA : O<sub>3</sub>-DMA (weight ratio, 1 : 1) determined an increase of the conversion degree to about 85% [(Figure 6(a)]. This experimental evidence demonstrates that the urethane oligomer mixture (cinnamate dimethacrylate/

PTHF dimethacrylate) is more reactive than O<sub>1</sub>-DMA, but less reactive than O<sub>3</sub>-DMA (DC, 95%). The graphical representation of the maximum photopolymerization rate versus time [Figure 6(b)] showed that the incorporation of O<sub>3</sub>-UDMA (viscosity,  $\sim 6.2 \text{ Pa s}$ ) into the macromer mixture determined a small decrease of the polymerization rate (from  $R_p = 0.101 \text{ s}^{-1}$  in O<sub>1</sub>-DMA to  $R_p = 0.090 \text{ s}^{-1}$  in O<sub>1</sub>-DMA/O<sub>3</sub>-DMA). The reason of this minor decrease is not clear, but we considered that the obtained results are in good agreement to those reported in the literature.<sup>47</sup>

At this point, it should be mentioned that the nonpolymerizable derivative, C-DOH used in the synthesis of urethane oligomers do not induce thermal transitions (data not shown), proving that the obtained photo-DSC data are exclusively related to polymerization reaction. It assumes that under the photo-DSC-specified irradiation conditions (low intensity), the cinnamate moieties exert predominantly steric effects on the polymerizability of the methacrylate C=C bond and chain growth. This result is consistent with the measurements made through UV spectroscopy, which indicated the lack of any modification in the UV spectrum of O<sub>1</sub>-DMA even after 5 min of exposure to visible light of higher intensity ( $800 \text{ mW/cm}^2$ ).

Influence of photoinitiator type and temperature on the photopolymerization manner was further investigated by examining the conversion and rate profiles of O<sub>1</sub>-DMA (Figure 7), observing that the photoreactivity undergoes changes under UV irradiation. Thus, it was found that the DC at 25°C was higher in the system containing 1.5 wt % Darocur TPO (DC, 74%) than that determined in the presence of Irgacure 651 (DC, 61.2%) or camphorquinone/amine (DC, 59.5%), whereas the polymerization rate decreased from  $0.096 \text{ s}^{-1}$  (Darocur TPO) to  $0.038 \text{ s}^{-1}$  (CQ/DMPheAA) (Figure 7(a) and Table I). These remarks suggested that the most effective photoinitiator for the studied system is Darocur TPO. Then, varying the polymerization temperature in the range of 25–60°C, the conversion degree (DC, 89.6%) and polymerization rate ( $0.155 \text{ s}^{-1}$ ) increased after photopolymerization of O<sub>1</sub>-DMA with 1.5 wt % Darocur TPO at

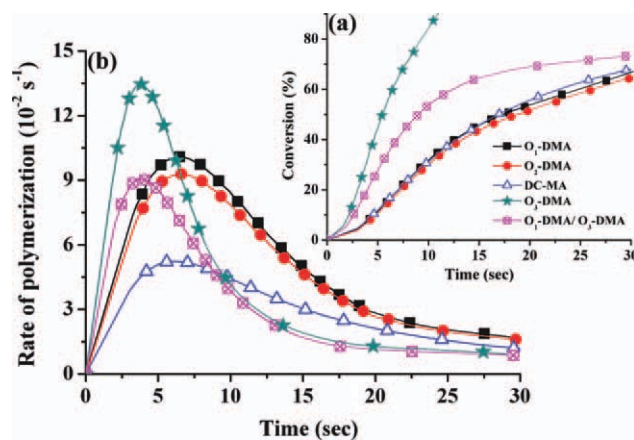


Figure 6. Double-bond conversion (a) and polymerization rate ( $R_p$ ) (b) as a function of irradiation time for urethane monomers in the presence of 1 wt % Darocur TPO. [Color figure can be viewed in the online issue, which is available at [wileyonlinelibrary.com](http://wileyonlinelibrary.com).]

**Table I.** Photo-DSC Data of Cinnamate Monomers Alone or in Combination With Urethane Dimethacrylate O<sub>3</sub>-DMA, Using Different Photoinitiators at Temperatures Between 25 and 60°C

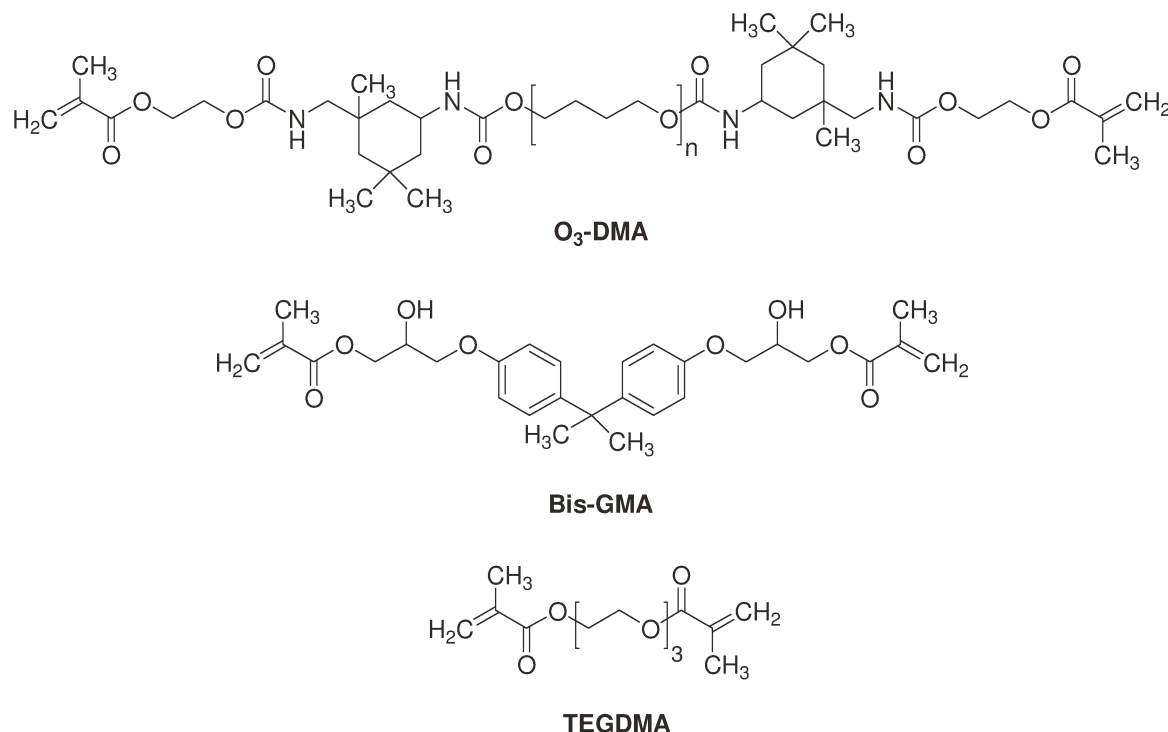
Initiator system	Sample	Conversion (%)	$\Delta H$ (J/g)	$t_{\max}$ (sec)	Polymerization rate ( $R_p$ ) (s <sup>-1</sup> )
1% Darocur TPO (25°C)	O <sub>1</sub> -DMA	70.4	75.8	6.5	0.101
1% Darocur TPO (25°C)	O <sub>2</sub> -DMA	68	72.4	6.6	0.093
1% Darocur TPO (25°C)	DC-MA	94	99.7	6.2	0.052
1% Darocur TPO (25°C)	O <sub>3</sub> -DMA	95	61.6	3.8	0.134
1% Darocur TPO (25°C)	O <sub>1</sub> -DMA/O <sub>3</sub> -DMA	84.7	73	3.8	0.090
0.75/1.5% CQ/DMPheAA (25°C)	O <sub>1</sub> -DMA	59.5	64.06	9	0.038
1.5% Irgacure 651 (25°C)	O <sub>1</sub> -DMA	61.2	65.92	4	0.092
1.5% Darocur TPO (25°C)	O <sub>1</sub> -DMA	74	79.7	3.5	0.096
1.5% Darocur TPO (40°C)	O <sub>1</sub> -DMA	86.2	92.8	3	0.129
1.5% Darocur TPO (60°C)	O <sub>1</sub> -DMA	89.6	96.5	2.5	0.155

60°C [Figure 7(b)]. This behavior encountered in photopolymerization of the O<sub>1</sub>-DMA dimethacrylate can be explained in terms of molecular mobility of the oligomeric chains that is highly enhanced by rising the temperature when the diffusion-controlled free radical polymerization occurs.

**Properties of Composite Resins.** To evaluate the specific properties of some hybrid composites, acrylic resins were prepared by photopolymerization upon exposure to visible light of the mixture of Bis-GMA, TEGDMA, and cinnamate monomers, using the CQ/amine initiator system, according to the gravimetric compositions summarized in Table II. Each formulation (F1–F3) contains 25 wt % organic phase and 75 wt % inorganic filler. The organic phase consists of cinnamate monomer (20 wt

%), Bis-GMA (48.5 wt %), TEGDMA (30 wt %), and photoinitiator (0.5% CQ/1 % DMPheAA). After the incorporation of quartz glass, the photocurable pastes were crosslinked with a dental photopolymerization lamp (light intensity, 800 mW/cm<sup>2</sup>; 60 s). For comparison, another specimen based on O<sub>1</sub>-DMA/O<sub>3</sub>-DMA, Bis-GMA, and TEGDMA (F4) was prepared. Taking into account the probable effects of physicochemical structure of the polymeric matrix on the composite properties, the PS, water sorption/solubility, compressive, and DTSs were measured for F1–F4 photocurable samples.

The PS measured for polymer composites is a crucial parameter in determining the subsequent features of crosslinked matrixes, reason for that is assessment in the present study is important.

**Scheme 3.** Structures of monomers used in dental formulations.



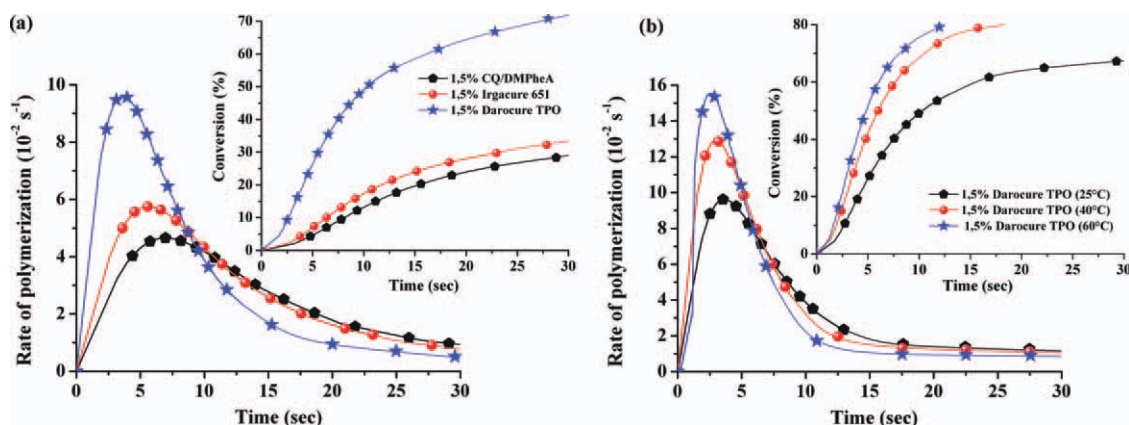


**Figure 7.** Photo-DSC profiles of oligodimethacrylate with cinnamate groups (O<sub>1</sub>-DMA) in the presence of various photoinitiators (a) and different temperatures (b). [Color figure can be viewed in the online issue, which is available at [wileyonlinelibrary.com](http://wileyonlinelibrary.com).]

Thus, from the data summarized in Table II it can be remarked that the samples containing O<sub>1</sub>-DMA (F2, PS = 6.4 vol %) or O<sub>2</sub>-DMA (F3, PS = 6.1 vol %) showed a lower PS than that of the sample in which there is low-molecular-weight monomer DC-MA (F1, PS = 8.2 vol %), their partners remaining unchanged. From the displayed results, one can appreciate that the values of PS for the composites achieved with cinnamate monomers, especially oligomers, are better than those measured for Bis-GMA/TEGDMA (70/30 wt %) mixture without filler (PS = 7.04 vol %).<sup>48</sup> In connection, the PS determined for F4 formulation based on O<sub>1</sub>-DMA/O<sub>3</sub>-DMA had a close value (6.3 vol %) to the oligodimethacrylate alone, resulting from a tightly packing of the polymer network after polymerization. Considering the photobehavior of cinnamate monomers, it is clear that lower shrinkage and higher conversion, which are inherent to polymerization reactions, are normally in opposite relationship, but such a finding is not new in the case of dental materials.<sup>49,50</sup>

Useful information about the properties and capacity of these materials to be employed as dental resin composites is provided by specific analyses. Hence, for the hybrid composites resulted by the inclusion of cinnamate (di)methacrylates along with commercial monomers and an important amount of filler, the wetting characteristics were determined by means of contact

angle ( $\theta$ ) method. The contact angle measurements for distilled water (Table II) indicated that the composite F1 containing DC-MA monomer presents a hydrophobic surface ( $\theta = 104^\circ$ ), whereas the hybrid composites having PEG (PPG) polyether sequences in the structure exhibited moderately hydrophilic surfaces (F2,  $\theta = 73^\circ$ ; F3,  $\theta = 76^\circ$ ). These results showed that the incorporation of soft segments into the photopolymerizable formulation had as effect a decrease of the water contact angle on the surface of the composite resins. In the case of composite F4 that contains the mixture O<sub>1</sub>-DMA/O<sub>3</sub>-DMA, contact angle had a value of  $\theta = 81^\circ$ , close to that found for the composites with cinnamate oligodimethacrylates, suggesting that the presence of poly(THF) does not alter the wetting properties of the composite resins.

Another significant feature characterizing the hybrid composites is water sorption, a diffusion-controlled process that primarily depends on hydrophobicity and crosslinking density of the cured resins. The results of water sorption in Figure 8 show that the discussed resin composites have water sorption values ranging from 1.23 to 1.3 wt %. Analyzing these data, it is clear

**Table II.** Compositions (wt %), contact angle, and Polymerization Shrinkage of Some Dental Specimens Based on Cinnamate Monomers and Conventional Comonomers

Sample	Monomer (20%)	Bis-GMA (%)	TEGDMA (%)	Contact angle (°)	PS <sup>a</sup> (%)
F1	DC-MA	48.5	30	104	8.2
F2	O <sub>1</sub> -DMA	48.5	30	73	6.44
F3	O <sub>2</sub> -DMA	48.5	30	76	6.1
F4	O <sub>1</sub> -DMA/O <sub>3</sub> -DMA (1 : 1)	48.5	30	81	6.3

<sup>a</sup>Polymerization shrinkage determined by picnometry (in the absence of filler).

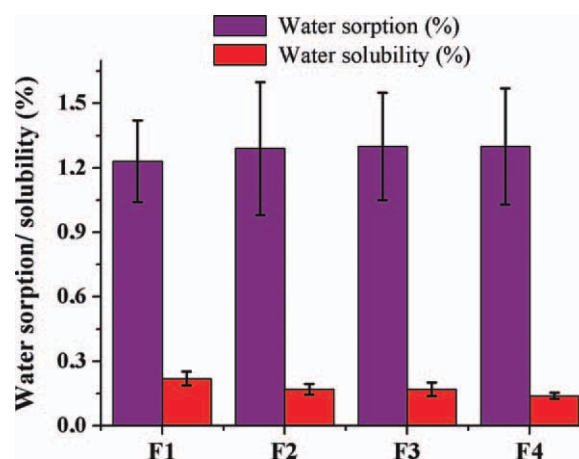


**Figure 8.** Percent of water sorption and water solubility for the prepared resin composites (error bar mean average standard deviations). [Color figure can be viewed in the online issue, which is available at [wileyonlinelibrary.com](http://wileyonlinelibrary.com).]

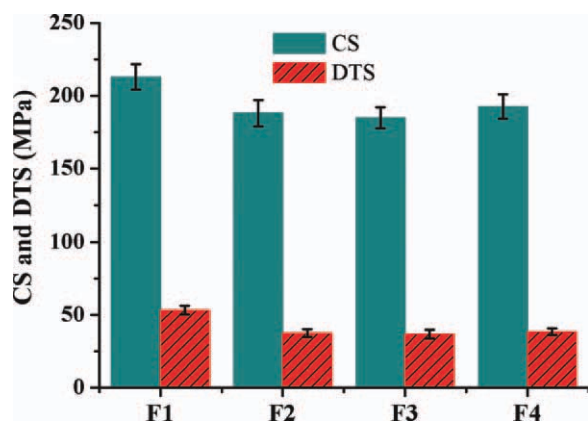


**Figure 9.** Compressive and DTSs determined for resin composites containing cinnamate monomers (error bar mean average standard deviations). [Color figure can be viewed in the online issue, which is available at [wileyonlinelibrary.com](http://wileyonlinelibrary.com).]

that the more hydrophilic composites showed a higher amount of absorbed water, whereas the leaching of small molecules in the presence of water occurred more intensively into the composite based on DC-MA monomer (F1), for which a water solubility of 0.22 wt % was determined.

The mechanical properties of these composites were expressed through DTS and CS. The mechanical tests performed on experimental composites containing cinnamate monomers, Bis-GMA, and TEGDMA, with a filler load of 75 wt % (quartz glass) exhibited better results for F1 (DTS, 53.2 MPa; CS, 212.9 MPa) than those of cured resins F2–F4 based on oligodimethacrylates (DTS, 36.9–38.5 MPa; CS, 185.0–192.6 MPa) that led to lower mechanical strengths (Figure 9). Note that the comparison between the DTS values found in the case of our composites and those obtained on materials based on Bis-GMA/TEGDMA (70 : 30) is in reasonable agreement.<sup>51</sup> Therefore, the presence of urethane structures into the above composites did not produce an increase in the strength and this result was surprising for our dimethacrylates, as the urethane sequences are recognized for their propensity to facilitate a strong interaction via hydrogen bonds.<sup>52</sup> In the same time, the DC and the relatively flexible nature of the resulting polymers could explain the mechanical parameters of these materials, without neglecting the filler component and the hand-mixing process used to prepare the experimental composites.

## CONCLUSIONS

Urethane dimethacrylates bearing PEG (PPG) flexible sequences and cinnamate units between the photopolymerizable groups were prepared and used in potential dental composites. Formation of the urethane oligocinnamates was demonstrated by <sup>1</sup>H NMR, <sup>13</sup>C NMR, UV/vis, and FTIR spectroscopies, GPC, ESI-MS analysis, and viscosity determinations. Compared to a low molecular-weight dicinnamate monomethacrylate, photopolymerization experiments performed by photo-DSC showed that the DC of methacrylic function depend on the monomer and photoinitiator structure (Darocour TPO, Irgacure 651, and CQ/amine), temperature, viscosity, and monomer composition. Sub-

sequently, the DC increased from 68% (oligocinnamate) to 94% (monomethacrylate), whereas the maximum polymerization rate was higher in the case of oligomers ( $R_{\max}^p : \sim 0.1 \text{ s}^{-1}$ ) comparatively with that of the low-molecular-weight monomer ( $R_{\max}^p : \sim 0.05 \text{ s}^{-1}$ ). Furthermore, PS of a mixture based on cinnamate monomer (20 wt %) and Bis-GMA, TEGDMA, and CQ/amine exposed to visible irradiation (light intensity, 800 mW/cm<sup>2</sup>) was lower in the specimens that contain photoactive oligomers, and is better than that determined for Bis-GMA/TEGDMA (70 : 30). With the addition of 75 wt % quartz glass, the surface properties measured for few photo-cured composites are similar to other materials based on Bis-GMA, but at the same time the mechanical properties (compressive and DTSs) are most probably the result of the quartz filler and the different structures of cinnamate monomers used in each formulation. However, for the best balance of the later, further investigation is needed.

## ACKNOWLEDGMENTS

The authors acknowledge the financial support of the CNCS-UEFISCDI through a project from the National Research Program (PN-II-ID-PCE 2011-3-0164; No. 40/5.10.2011).

## REFERENCES

- Pfeifer, C. S.; Silva, L. R.; Kawano, Y.; Braga, R. R. *Dent. Mater.* **2009**, *25*, 1136.
- Sideridou, I. D.; Karabela, M. M.; Vouvoudi, E. C.; Papanastasiou, G. E. *J. Appl. Polym. Sci.* **2008**, *107*, 463.
- Song, J.; Zhao, J.; Ding, Y.; Chen, G.; Sun, X.; Sun, D.; Li, Q. *J. Appl. Polym. Sci.* **2012**, *124*, 3334.
- Podgórski, M. *Dent. Mater.* **2010**, *26*, e188.
- Moszner, N.; Salz, U. *Macromol. Mater. Eng.* **2007**, *292*, 245.
- Gao, Y.; Sagi, S.; Zhang, L.; Liao, Y.; Cowles, D. M.; Sun, Y.; Fong, H. *J. Appl. Polym. Sci.* **2008**, *110*, 2063.
- Wang, Y.; Lee, J. J.; Lloyd, I. K.; Wilson, O. C.; Rosenblum, M.; Thompson, V. J. *Biomed. Mater. Res.* **2007**, *82A*, 651.
- Palin, W. M.; Fleming, G.; Nathwani, H.; Burke, T.; Randall, R. C. *Dent. Mater.* **2005**, *21*, 324.
- Lambrechts, P.; Goovaerts, K.; Bharadwaj, D.; De Munck, J.; Bergmans, L.; Peumans, M.; Van Meerbeek, B. *Wear* **2006**, *261*, 980.
- Michelsen, V. B.; Moe, G.; Strom, M. B.; Jensen, E.; Lygre, H. *Dent. Mater.* **2008**, *24*, 724.
- Satsangi, N.; Rawls, H. R.; Norling, B. K. *J. Biomed. Mater. Res. B Appl. Biomater.* **2005**, *74B*, 706.
- Boland, E. J.; Carnes, D. L.; MacDougall, M.; Satsangi, N.; Rawls, R.; Norling, B. *J. Biomed. Mater. Res. B Appl. Biomater.* **2006**, *79B*, 1.
- Buruiana, T.; Melinte, V.; Costin, G.; Buruiana, E. C. *J. Polym. Sci. A Polym. Chem.* **2011**, *49*, 2615.
- Matinlinna, J. P.; Lassila, L. V. J.; Kangasniemi, I.; Yli-Urpo, A.; Vallittu, P. K. *Dent. Mater.* **2005**, *21*, 287.
- Pavlinec, J.; Moszner, N. *J. Appl. Polym. Sci.* **2009**, *113*, 3137.

16. Moszner, N.; Gianasmidis, A.; Klapdohr, S.; Fischer, U. K.; Rheinberger, V. *Dent. Mater.* **2008**, *24*, 851.
17. Xiong, J.; Sun, X.; Li, Y.; Chen, J. *J. Appl. Polym. Sci.* **2011**, *122*, 1882.
18. Li, Y.; Sun, X.; Chen, J.; Xiong, J.; Hu, X. *J. Appl. Polym. Sci.* **2012**, *124*, 436.
19. Sahin, G.; Albayrak, A. Z.; Bilgici, Z. S.; Avci, D. *J. Polym. Sci. A Polym. Chem.* **2009**, *47*, 1953.
20. Moszner, N.; Fischer, U. K.; Angermann, J.; Rheinberger, V. *Dent. Mater.* **2008**, *24*, 694.
21. Kerby, R. E.; Knobloch, L. A.; Schrickler, S.; Gregg, B. *Dent. Mater.* **2009**, *25*, 302.
22. Chen, C.-Y.; Huang, C.-K.; Lin, S.-P.; Hsieh, K.-H.; Lin, C.-P. *Comput. Sci. Technol.* **2008**, *68*, 2811.
23. Ferracane, J. L. *Dent. Mater.* **2011**, *27*, 29.
24. Buruiana, E. C.; Buruiana, T.; Melinte, V.; Zamfir, M.; Colceriu, A.; Moldovan, M. *J. Polym. Sci. A Polym. Chem.* **2007**, *45*, 1956.
25. Buruiana, T.; Melinte, V.; Stroea, L.; Buruiana, E. C. *Polym. J.* **2009**, *41*, 978.
26. Buruiana, T.; Buruiana, E. C.; Melinte, V.; Colceriu, A.; Moldovan, M. *Polym. Eng. Sci.* **2009**, *49*, 1127.
27. Buruiana, T.; Melinte, V.; Jitaru, F.; Aldea, H.; Buruiana, E. C. *J. Compos. Mater.* **2012**, *46*, 371.
28. Buruiana, T.; Melinte, V.; Hitruc, G.; Buruiana, E. C. *Rev. Roum. Chim.* **2010**, *55*, 963.
29. Hayakama, T.; Takahashi, K.; Kikutake, K.; Yokoto, I.; Nemoto, K. *J. Oral. Sci.* **1999**, *41*, 9.
30. Peutzfeldt, A. *Eur. J. Oral. Sci.* **1997**, *105*, 97.
31. Sideriu, I.; Tserki, V.; Papanastasiou, G. *Biomaterials* **2002**, *23*, 1819.
32. Antonucci, J. M.; Regnault, W. F.; Skrtic, D. *J. Comput. Mater.* **2010**, *44*, 355.
33. Dart, E. C.; Perry, A. R.; Nemcek, J. US Pat. 4,110,184, August 29, **1978**.
34. Sung, S.-J.; Cho, K.-Y.; Yoo, J.-H.; Kim, W. S.; Chang, H.-S.; Cho, I.; Park, J.-K. *Chem. Phys. Lett.* **2004**, *394*, 238.
35. Buruiana, E. C.; Jitaru, F.; Buruiana, T.; Olaru, N. *Des. Monom. Polym.* **2010**, *13*, 167.
36. Sharma, P. *J. Chem. Pharm. Res.* **2011**, *3*, 403.
37. De, P.; Baltas, M.; Bedos-Belval, F. *Curr. Med. Chem.* **2011**, *18*, 1672.
38. Buruiana, E. C.; Jitaru, F.; Matei, A.; Dinescu, M.; Buruiana, T. *Soft Mater* **2011**, DOI: 10.1080/1539445X.2011.608101.
39. Wang, D.; Carrera, L.; Abadie, M. J. M. *Eur. Polym. J.* **1993**, *29*, 1379.
40. Sahin, G.; Avci, D.; Karahan, O.; Moszner, N. *J. Appl. Polym. Sci.* **2009**, *114*, 97.
41. Tarle, Z.; Meniga, A.; Risti, M.; Sutalo, J.; Pichler, G. *Croat. Chem. Acta* **1998**, *71*, 777.
42. Domingo, C.; Arcis, R. W.; Osorio, E.; Osorio, R.; Fanovich, M. A.; Rodriguez-Clemente, R.; Toledano, M. *Dent. Mater.* **2003**, *19*, 478.
43. Krol, P. *Prog Mater Sci* **2007**, *52*, 915.
44. Lemon, M. T.; Jones, M. S.; Stansbury, J. W. *J. Biomed. Mater. Res.* **2007**, *83A*, 734.
45. Sideridou, I. S.; Achilias, D. S.; Karava, O. *Macromolecules* **2006**, *39*, 2072.
46. Buruiana, T.; Melinte, V.; Chibac, A.; Matiut S.; Balan, L. *J. Biomater. Sci. Polym. Ed.* **2012**, *23*, 955.
47. Kilambi, H.; Cramer, N. B.; Schneidewind, L. H.; Shah, P.; Stansbury, J. W.; Bowman, C. N. *Dent. Mater.* **2009**, *25*, 33.
48. Kim, J. W.; Kim, L. U.; Kim, C. K.; Cho, B. H.; Kim, O. Y. *Biomacromolecules* **2006**, *7*, 154.
49. Labella, R.; Davy, K. W. M.; Lambrechts, P.; Van Meerbeek, B.; Vanherle, G. *Eur. J. Oral. Sci.* **1998**, *106*, 816.
50. Yagci, B.; Ayfer, B.; Albayrak, A. Z.; Avci, D. *Macromol. Mater. Eng.* **2006**, *291*, 336.
51. Jeon, M. Y.; Yoo, S. H.; Kim, J. H.; Kim, C. K.; Cho, B. H. *Biomacromolecules* **2007**, *8*, 2571.
52. Yilgor, E.; Yilgor, I.; Yurtsever, E. *Polymer* **2002**, *43*, 6551.
53. Kleverlaan, C. J.; Feilzer, A. *J. Dent. Mater.* **2005**, *21*, 1150.